Biochemistry

 Volume 42, Number 30 August 5, 2003

Articles

Effects of Photosynthetic Reaction Center H Protein Domain Mutations on Photosynthetic Properties and Reaction Center Assembly in *Rhodobacter sphaeroides*†

Ali Tehrani,‡ Roger C. Prince,§ and J. Thomas Beatty*,‡

Department of Microbiology and Immunology, University of British Columbia, 300-6174 University Boulevard, Vancouver, BC, Canada, V6T 1Z3, and ExxonMobil Research and Engineering Company, 1545 Route 22 East, Annandale, New Jersey 08801

Received April 28, 2003; Revised Manuscript Received May 27, 2003

ABSTRACT: Purple bacterial photosynthetic reaction center (RC) H proteins comprise three cellular domains: an 11 amino acid N-terminal sequence on the periplasmic side of the inner membrane; a single transmembrane α-helix; and a large C-terminal, globular cytoplasmic domain. We studied the roles of these domains in *Rhodobacter sphaeroides* RC function and assembly, using a mutagenesis approach that included domain swapping with *Blastochloris viridis* RC H segments and a periplasmic domain deletion. All mutations that affected photosynthesis reduced the amount of the RC complex. The RC H periplasmic domain is shown to be involved in the accumulation of the RC H protein in the cell membrane, while the transmembrane domain has an additional role in RC complex assembly, perhaps through interactions with RC M. The RC H cytoplasmic domain also functions in RC complex assembly. There is a correlation between the amounts of membrane-associated RC H and RC L, whereas RC M is found in the cell membrane independently of RC H and RC L. Furthermore, substantial amounts of RC M and RC L are found in the soluble fraction of cells only when RC H is present in the membrane. We suggest that RC M provides a nucleus for RC complex assembly, and that a RC H/M/L assemblage results in a cytoplasmic pool of soluble RC M and RC L proteins to provide precursors for maximal production of the RC complex.

Purple phototrophic bacteria have provided a wealth of information on fundamental aspects of electron- and proton-transfer reactions catalyzed by membrane-integral pigment−protein complexes (*1*, *2*). In *Rhodobacter sphaeroides*, light is absorbed by light-harvesting antennae called LH2 and LH1 and transferred to the reaction center (RC)[1] complex, which operates as a light-driven two-electron/two-proton quinone reductase. Electrons are transferred from a special pair of bacteriochlorophylls (sometimes called D) through the quinone Q_A to a second RC-bound quinone called Q_B, and protons are translocated from the cytoplasm to Q_B to produce a quinol. The Q_B quinol leaves the RC and is oxidized at the periplasmic side of the cytochrome b/c_1 complex, resulting in the net translocation of protons from inside to outside the cell membrane, while electrons are transferred from the b/c_1 complex to the RC (*3*, *4*). Thus, a cycle of

† This research was supported by a grant from the CIHR to J.T.B.

* Address correspondence to the following author. Phone: (604) 822-6896. Fax: (604) 822-6041. E-mail: jbeatty@interchange.ubc.ca.

‡ University of British Columbia.

§ ExxonMobil Research and Engineering Company.

[1] Abbreviations: BChl, bacteriochlorophyll; D, reaction center special pair of bacteriochlorophylls; LH1, light-harvesting complex 1; LH2, light-harvesting complex 2; Q_A, reaction center quinone A; Q_B, reaction center quinone B; RC, reaction center; SDS−PAGE, sodium dodecyl sulfate polyacrylamide gel electrophoresis.

10.1021/bi0346650 CCC: $25.00
Published on Web 07/10/2003

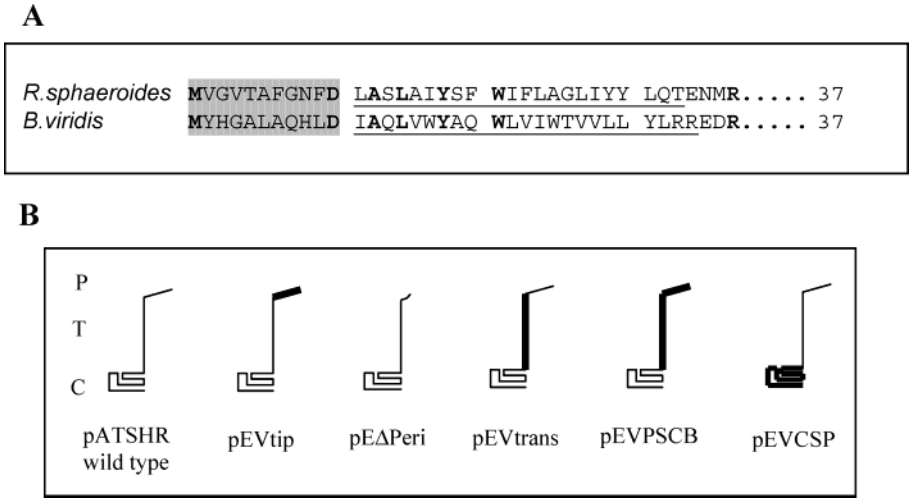

FIGURE 1: (A) Amino acid alignment of *R. sphaeroides* and *B. viridis* RC H N-terminal sequences. Shaded area indicates periplasmic amino acids, and underlined residues form an α-helix that spans the membrane. Identical amino acids are in bold, and the number 37 refers to a conserved R residue. (B) Representation of the RC H proteins (with respective plasmid names provided below each) used in this study. P = periplasmic domain; T = transmembrane domain; and C = cytoplasmic domain. Thick lines indicate *B. viridis* sequences.

electron-transfer reactions is coupled to the formation of a proton gradient across the cell membrane, and this gradient is used by the cell to produce ATP and drive other cell processes.

X-ray crystallography of LH2 complexes revealed symmetrical pigment−protein ring structures (*5*, *6*), which transfer light energy to the LH1 complex (*7*). The LH1 complex transfers light energy to the RC, and a variety of experiments indicate the existence of a core LH1/RC supercomplex in which LH1 more or less encircles the RC (*8*, *9*).

High-resolution crystal structures of the RCs of *Blastochloris viridis* (formerly *Rhodopseudomonas viridis*) and *R. sphaeroides* are very similar (*10*) and contain three proteins called RC H, RC M, and RC L. RC M and RC L each have five transmembrane segments that bind bacteriochlorophyll (BChl) and other cofactors. RC H does not interact directly with cofactors and can be conceptually divided into three domains: (1) a ∼11 amino acid N-terminal domain located on the periplasmic side of the inner membrane of these Gram-negative bacteria; (2) a single transmembrane α-helix; and (3) a C-terminal, large, globular cytoplasmic domain (*10*). Despite the very similar polypeptide backbone folding, the overall amino acid sequence identity in alignments is only ∼38% (not shown).

Removal of the RC H protein from the *R. sphaeroides* RC in vitro destabilized the Q_B quinone, although electron transfer from D to Q_A still occurred (*11*). Gross disruptions of the RC H gene rendered the RC undetectable in absorption spectra and abolished photosynthetic growth in several species, although traces of RC primary charge separation were reported in *R. sphaeroides* and *Rhodospirillum rubrum* mutants. Interestingly, these RC H gene disruptions reduced the levels of the LH1 complex (*12*−*15*). It was suggested that the RC H protein is required in vivo to provide chaperone-like activities for membrane insertion of the RC M and RC L proteins to form the RC holocomplex (*14*, *16*) and that this holocomplex is required for maximal levels of LH1 (*13*, *15*, *17*). However, the details of how the RC H protein might participate in these proposed activities, and which segment(s) of the protein are involved, were unknown.

Most site-directed mutagenesis studies of the RC have focused on RC L and RC M, in part because experiments on RC H were hampered by the lack of an efficient system for in vivo production of mutant RC H proteins. We developed such a system and previously applied it to address questions about the pathway and mechanism of proton transfer through the RC H cytoplasmic domain (*12*, *18*−*20*).

This paper describes experiments in which the three domains of the *R. sphaeroides* RC H protein were replaced with the corresponding segments from the *B. viridis* protein. Amino acid substitutions and a deletion in the *R. sphaeroides* RC H periplasmic domain were also created. The effects of these mutations were evaluated in terms of photosynthetic growth, steady-state absorption spectra, light-driven electron- and proton-transfer reactions, and Western blot analyses of RC proteins in cellular membrane and soluble fractions. The results indicate that all three RC H domains affect the amount of RC H (and the RC complex) in the cell membrane. The amount of membrane-associated RC L (but not RC M) parallels the amount of RC H, and the presence of membrane-associated RC H is needed to establish a cytoplasmic pool of RC M and RC L. We suggest a preliminary model for the assembly of the protein components of the RC complex.

MATERIALS AND METHODS

Bacterial Strains and Plasmids. Table 1 lists the strains and plasmids. The *R. sphaeroides* RC H gene in plasmid pTZ18U::puhA was subcloned as a 1.3-kb *Bam*H I fragment into pATP19P, yielding plasmid pATSHR. The *B. viridis* RC H gene of plasmid pDG4B was transferred to pTZ18U as a *Bam*H I to *Xma* III fragment; subcloned into pUC19 as a 1.5-kb *Eco*R I fragment, yielding plasmid pUC19::vpuhA; and transferred from pUC19::vpuhA as an *Eco*RI fragment to pATP19P to yield pATVHR.

Site-directed sequence changes were introduced by use of the QuikChange kit (Stratagene), and all mutations were DNA sequenced. Several intermediate plasmids were used to create the mutant RC H expression vectors as described later. The proteins produced by each of the mutants are represented in Figure 1B.

Table 1: Bacterial Strains and Plasmids

strains or plasmids	relevant characteristics	source or ref
	Strains	
E. coli		
DH5α	F$^-$, Δ(*lac*ZYA-*arg*F) *deo*R, *rec*A1, *end*A1	Invitrogen
DH10B	F$^-$, *mcr*A, *rec*A1, *end*A1, *ara*Δ 139, Δ*lac*X74	Invitrogen
HB101(pRK2013)	pRK2013 contains RK2 transfer genes	*21*
R. sphaeroides		
ΔPUHA	RC$^-$, LH1$^+$, LH2$^+$	*12*
ΔPUHAΔPUC	RC$^-$, LH1$^+$, LH2$^-$, Kan^r	*18*
	Plasmids	
pAli::puhA	pTZ::puhA with *Hin*d III to *Xba* I of the multiple cloning site removed	this paper
pATP19P	pRK415 containing *R. sphaeroides puc* promoter as a 0.75 kb *Hin*d III fragment	*20*
pATSHR	pATP19P containing *Bam*H I fragment of pTZ18U::puhA	this paper
pATVHR	pATP19P containing *R. viridis* RC H gene as a 1.5 kb *Eco*RI fragment	this paper
pDG4B	contains *B. viridis* RC H gene as 3.5 kb *Bam*HI fragment	J. Farchaus
pΔPeri	pTemp2 with codons G-3 through F-10 removed	this paper
pEΔPeri	pATP19P containing the *Bam*H I fragment of pΔPeri	this paper
pEVPSCB	pATP19P containing the *Eco*R I fragment of pVPSCB	this paper
pEVCSP	pATP19P containing the *Bam*H I fragment of pVCSP	this paper
pEVtrans	pATP19P containing the *Bam*H I fragment of pVtrans	this paper
pEVtip	pATP19P containing the *Bam*H I fragment of pVtip	this paper
pRK415	broad host-range cloning vector, Tc^r	*33*
pTemp2	pAli::puhA with two *Hinc* II sites engineered at G-3 and F-10/D-11 codons	this paper
pTZ18U	cloning vector, Ap^r	Pharmacia
pTZ18U::mspuhA	pTZ18U::puhA with an engineered *Dde* I site at T-33 codon	this paper
pTZ18U::puhA	pTZ18U containing the *R. sphaeroides* RC H gene as a 1.34 kb *Bam*H I fragment	*12*
pTZ18U::puhA2.1	pTZ18U::puhA with an engineered *EcoR* V site at L-12 codon	this paper
pTZ18U::xbsph	pTZ18U::puhA with an engineered *Xba* I site at F-10	this paper
pUC19	cloning vector, Ap^r	*34*
pUC19::mvpuhA	pUC19::vpuhA with an engineered *Dde* I site at R-34 codon	this paper
pUC19::vpuhA	pUC19 containing the *B. viridis* RC H gene as a 1.5 kb *Eco*R I fragment	this paper
pUC19::xbvir	pUC19::vpuhA with an engineered *Xba* I site at L-10	this paper
pVCSP	pUC19 encoding RCH gene with the *B. viridis* cytoplasmic residues (starting at Glu 35) in place of the *R. sphaeroides* sequence (after Glu 34) as a 1.4 kb *Bam*H I fragment	this paper
pVPSCA	pUC19 containing a RC H gene encoding the *B. viridis* periplasmic and transmembrane domains (has P as 34th codon) and the *R. sphaeroides* cytoplasmic domain	this paper
pVPSCB	pVPSCA with P-34 changed to R (wild type)	this paper
pVPSCB2	pVPSCB with an engineered *Eco*R V site at D-11 codon	this paper
pVtip	pUC19 containing a hybrid RC H gene encoding the *B. viridis* periplasmic amino acids in place of the corresponding *R. sphaeroides* sequence as a 0.9 kb *Bam*H I fragment	this paper
pVtrans	pTZ18U containing a hybrid *puhA* gene encoding the *B. viridis* transmembrane domain flanked by the *R. sphaeroides* periplasmic and cytoplasmic domains as a 1.2 kb *Bam*H I fragment	this paper

The plasmid pEVtip encodes the *B. viridis* periplasmic amino acids Met-1 to Asp-11 in place of the corresponding *R. sphaeroides* sequence (see shaded residues in Figure 1A). To construct the plasmid pEVtip, *Xba* I sites were engineered

at the RC H Leu-10 codon (TTA → CTA) of plasmid pUC19::vpuhA, and Asn-9 (AAC → AAT) and Phe-10 (TTC → CTA) codons of plasmid pTZ18U::puhA, to yield the intermediate plasmids pUC19::xbvir and pTZ18U::xbsph, respectively (both plasmids also contain *Xba* I sites 5′ of their respective RC H genes). After an *Xba* I digest, the 845-bp DNA fragment from plasmid pTZ18U::xbsph was ligated to a 2.7-kb fragment from the plasmid pUC19::xbvir, resulting in plasmid pVtip. The hybrid RC H gene in plasmid pVtip was subcloned as a 900-bp *Bam*H I fragment into the expression vector pATP19P to yield pEVtip.

Plasmid pEΔPeri encodes a mutant *R. sphaeroides* RC H protein in which Val-2 is followed by Asp-11 (codons 3−10 of the RC H periplasmic domain were removed; see Figure 1A). Plasmid pEΔPeri was made by first introducing two *Hin*c II restriction sites, one at the Gly-3 codon (GGT → AAC) and the other at the Phe-10/Asp-11 codons (TTC/GAT to GTC/GAC) in plasmid pTZ18U::puhA, resulting in plasmid pTemp2. After *Hinc* II digestion, the DNA segment encoding Gly-3 to Phe-10 was removed, and the plasmid was religated to yield plasmid pΔPeri. A 1.3-kb *Bam*H I fragment from pΔPeri encoding the mutant RC H gene was subcloned into the expression vector pATP19P to obtain pEΔPeri.

Plasmid pEVtrans encodes the *R. sphaeroides* periplasmic domain from Met-1 to Asp-11, followed by the *B. viridis* transmembrane domain from Ile-12 to Arg-34 (Figure 1A), and the *R. sphaeroides* cytoplasmic domain from Glu-34 onward. This plasmid was created by initially introducing *Dde* I sites at the location corresponding to the junction between the transmembrane and the cytoplasmic domains of both the RC H genes in plasmids pUC19::vpuhA and pTZ18U::puhA. This was done by changing the *R. sphaeroides* Thr-33 codon (ACC → ACT) yielding plasmid pTZ18U::mspuhA and the *B. viridis* Arg-34 codon (CGT → CCT) to yield plasmid pUC19::mvpuhA. A 3.6-kb *Hin*d III (filled in with T4 DNA polymerase) to *Dde* I fragment containing the DNA sequence of the *R. sphaeroides* cytoplasmic domain was obtained from pTZ18U::mspuhA and ligated to a 240-bp *Pvu* II to *Dde* I fragment (encoding the *B. viridis* periplasmic and transmembrane domains) from pUC19::mvpuhA to yield plasmid pVPSCA. The DNA sequence of plasmid pVPSCA RC H codon 34 was changed from CCT back to CGT (restoring Arg-34), creating pVPSCB. *Eco*R V sites were introduced at the *B. viridis* RC H Asn-11 codon (GAC → GAT) in pVPSCB, to yield pVPSCB2, and at the *R. sphaeroides* RC H Leu-12 codon (CTG → ATC) in pTZ18U::puhA, yielding pTZ18U::puhA2.1. The 800-bp *Eco*R V to *Hin*d III fragment of pVPSCB2 was ligated to the 3.2-kb fragment of plasmid pTZ18U::puhA2.1, yielding pVtrans. A 1.4-kb *Bam*H I fragment was subcloned from pVtrans into pATP19P to yield pEVtrans.

To obtain plasmid pEVPSCB, which contains a RC H gene encoding the *B. viridis* periplasmic and transmembrane domains (Met-1 to Arg-34; see Figure 1A) followed by *R. sphaeroides* sequences from Glu-34 onward, the 1.4-kb *Eco*R I fragment from plasmid pVPSCB was subcloned into the expression vector pATP19P.

Plasmid pEVCSP encodes the *R. sphaeroides* RC H periplasmic and transmembrane domains (amino acids Met-1 to Glu-34; see Figure 1A) followed by the *B. viridis* RC H cytoplasmic domain (from Asp-36 onward). Plasmid pEVCSP was constructed by ligation of a 3.4-kb *Kpn* I (resected with T4 DNA polymerase) to *Dde* I fragment from pTZ18U::mspuhA to a 820-bp *Pvu* II to *Dde* I DNA fragment from pUC19::mvpuhA to yield plasmid pVCSP. The 1.4-kb *Bam*H I fragment from plasmid pVCSP was subcloned into pATP19P to yield pEVCSP. *Escherichia coli* strain DH10B and the *E. coli* helper strain HB101(pRK2013) were used for transfer of plasmids to *R. sphaeroides* in tri-parental conjugations (*21*).

Growth of Cultures. RCV medium (*22*) supplemented with 1 μg mL^{-1} nicotinic acid was used for the growth of *R. sphaeroides* at 30 °C. For semi-aerobic growth, cultures were grown in Erlenmeyer flasks filled to 80% of the nominal volume and shaken at 150 rpm. Photosynthetic cultures were inoculated with cells grown under semi-aerobic conditions and incubated in completely filled screw-cap tubes, illuminated with ∼275 μE m^{-2} s^{-1} of light from halogen lamps (Capsylite; Sylvania). *B. viridis* was grown photosynthetically in YPS medium (*23*).

For plasmid selection, media were supplemented with antibiotics at the following concentrations: *R. sphaeroides*, tetracycline-HCl at 2 μg mL^{-1} and kanamycin-sulfate at 25 μg mL^{-1}; and *E. coli*, tetracycline-HCl at 10 μg mL^{-1}, kanamycin-sulfate at 50 μg mL^{-1}, and ampicillin at 150 μg mL^{-1}. Turbidities of liquid cultures were measured with a Klett−Summerson colorimeter equipped with a red (#66) filter (1 Klett unit = ∼10^7 cells mL^{-1}).

Absorption Spectroscopy of Intact Cells. Cells of semi-aerobic cultures grown to ∼150 Klett units (∼72 h) were pelleted, resuspended in 0.25 mL of RCV medium, and mixed with 0.75 mL of a 30% bovine serum albumin solution to reduce light scattering. Spectral data were obtained on a TIDAS II spectrophotometer (World Precision Instruments) and analyzed using the J&M Spectralys program, version 1.82. Spectra were adjusted to the same 650 nm value, due solely to light scattering of suspended cells, to compensate for minor differences in concentrations.

Cell Fractionation. Cells from semi-aerobic *R. sphaeroides* cultures (or *B. viridis* grown photosynthetically) were pelleted, resuspended in 50 mM Tris-HCl buffer (pH 8.0), disrupted using a French pressure cell, and centrifuged at 25 800*g* for 10 min. The supernatant was centrifuged at 412 000*g* for 14 min to pellet membrane vesicles (chromatophores); the resuspended pellet and supernatant were centrifuged a second time, yielding the membrane fraction with the top 12% of the supernatant sample collected as the soluble protein fraction. The *B. viridis* RC was purified as described (*24*), and the *R. sphaeroides* purified RC sample was a generous gift from M. Paddock (University of California, San Diego). Samples were stored on ice for flash spectroscopy or at −80 °C for Western blots.

Flash Spectroscopy. Measurements were performed as previously described in a double-beam spectrophotometer (*25*). Chromatophore suspensions (A_{870} = 2.0) were reduced with 5 mM sodium ascorbate and allowed to equilibrate in the dark for at least 30 min before use, poising the ambient redox potential around E_h = +150 mV. The carotenoid bandshift (*26*) was measured at 490 minus 475 nm after a single actinic flash (10 μs full width at half-height, filtered through a Wratten 88A filter). The reaction center concentration was determined by the absorbance change at 605 minus

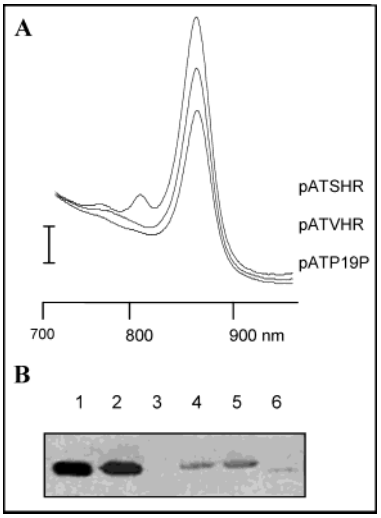

FIGURE 2: (A) Absorption spectra of ΔPUHAΔPUC (LH2$^-$) intact cells containing plasmids: top, pATSHR (*R. sphaeroides* RC H gene); middle, pATVHR (*B. viridis* RC H gene); bottom, pATP19P (expression vector lacking a RC H gene). The vertical bar indicates $A = 0.15$. (B) Western blot probed with *R. sphaeroides* RC H antiserum. Samples used were lane 1, purified *R. sphaeroides* RC (control); lane 2, chromatophores from ΔPUHAΔPUC(pATSHR); lane 3, chromatophores from ΔPUHAΔPUC(pATP19P); lane 4, purified *B. viridis* RC; lane 5, chromatophores from *B. viridis*; and lane 6, chromatophores from ΔPUHAΔPUC(pATVHR).

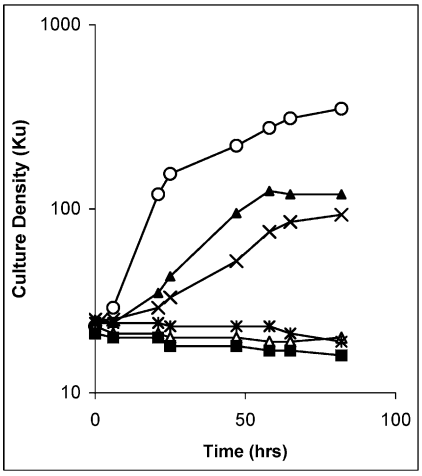

FIGURE 3: Photosynthetic growth of *R. sphaeroides* ΔPUHAΔPUC (LH2$^-$) cells containing the following plasmids: pATSHR (wild-type RC H, open circles); pEVtip (hybrid RC H containing *B. viridis* periplasmic domain, open triangles); pEΔPeri (mutant RC H lacking the periplasmic domain, filled squares); pEVtrans (hybrid RC H containing *B. viridis* transmembrane domain, filled triangles); pEVPSCB (hybrid RC H containing *B. viridis* periplasmic and transmembrane domains, crosses); and pEVCSP (hybrid RC H containing *B. viridis* cytoplasmic domain, asterisks). Ku, Klett units.

540 nm after a train of eight flashes separated by 32 ms, in the presence of 4 μM valinomycin and 1 μM antimycin (*27*).

Western Blotting. Chromatophores (10 μg of protein as determined by a modified Lowry method (*28*)) were mixed with SDS−PAGE sample buffer (*29*) and heated at 95 °C for exactly 1 min. Volumes of the soluble proteins proportional to the chromatophores in unfractionated extracts, and empirically determined amounts of pure RCs, were treated the same way. Samples were run on SDS−PAGE (12% acrylamide) and transferred to membranes, and the RC H, RC M, or RC L proteins were detected, all as recommended in the ECL Western blotting kit (Amersham Biosciences). The rabbit antisera raised against purified *R. sphaeroides* RC proteins were gifts, with the anti-RC H serum kindly provided by S. Kaplan (University of Texas) and the anti-RC M/L sera provided by E. Abresch (University of California, San Diego).

RESULTS

Development of the Experimental System. Plasmid pATVHR was used to express the *B. viridis* RC H gene in *R. sphaeroides* ΔPUHA (LH2$^+$) and ΔPUHAΔPUC (LH2$^-$) strains, which contain a translationally in-frame chromosomal deletion of the RC H gene. The complemented strains were incapable of photosynthetic growth, although expression of the *B. viridis* RC H gene was indicated by absorption spectra. For example, although the 760 and 804 nm RC peaks were absent from ΔPUHAΔPUC(pATVHR) cells (Figure 2A), the LH1 870 nm peak was greater than that of the strain that contained the expression plasmid pATP19P (which lacks a RC H gene), and the broad region of absorbance centered at 770 nm indicates protein-free BChl and/or degradation products.

The production of the *B. viridis* RC H protein in *R. sphaeroides* was also evaluated in Western blot experiments, using the *R. sphaeroides* RC H antiserum (Figure 2B). This antiserum reacted weakly with the RC H protein in purified *B. viridis* RC or chromatophore samples, but a band that was absent from the strain that contained pATP19P was obtained using chromatophores from the ΔPUHAΔPUC-(pATVHR) strain. We attribute this band to the *B. viridis* RC H protein, which migrated to a slightly lower MW position than in the *B. viridis* samples, and so perhaps the *B. viridis* RC H protein is proteolytically cleaved when present in *R. sphaeroides*.

The expression of the *B. viridis* RC H gene in *R. sphaeroides*, coupled with the absence of a functional RC complex, provided a system in which segments of these two structurally well-characterized RC H proteins could be exchanged or deleted (Figure 1B) to investigate RC H protein domain-specific functions, such as in RC complex catalytic activity and assembly.

Photosynthetic Growth of ΔPUHAΔPUC Strains Expressing Mutant RC H Genes. The LH2$^-$ strain ΔPUHAΔPUC was used in these experiments to allow comparison of growth properties with the RC and LH1 levels.

Strains containing plasmids encoding the periplasmic domain substitution or deletion (pEVtip and pEΔPeri, respectively) were incapable of photosynthetic growth (Figure 3).

Replacement of the transmembrane domain (pEVtrans) supported photosynthetic growth, although at a lower rate and to a lower final cell density than the wild-type control (Figure 3). The strain ΔPUHAΔPUC(pEVPSCB), which encodes a RC H protein consisting of the periplasmic and transmembrane domains of *B. viridis* RC H in place of *R. sphaeroides* sequences, grew photosynthetically with a rate and yield intermediate between the growth obtained when only the transmembrane or periplasmic domain was substituted. When the *R. sphaeroides* RC H cytoplasmic domain was replaced with the counterpart from *B. viridis* in pEVCSP, the resultant strain was incapable of photosynthetic growth (Figure 3). The poor photosynthetic growth of ΔPUHAΔPUC

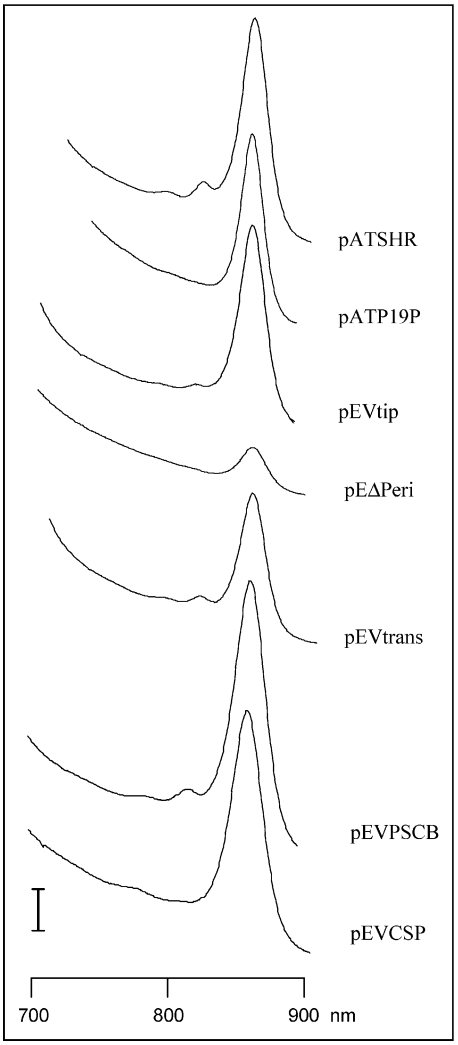

FIGURE 4: Absorption spectra of ΔPUHAΔPUC (LH2$^-$) intact cells containing the following plasmids: pATSHR (*R. sphaeroides* RC H); pATP19P (expression vector); pEVtip (hybrid RC H containing *B. viridis* periplasmic domain); pEΔPeri (mutant RC H lacking the periplasmic domain); pEVtrans (hybrid RC H containing *B. viridis* transmembrane domain); pEVPSCB (hybrid RC H containing *B. viridis* periplasmic and transmembrane domains); and pEVCSP (hybrid RC H containing *B. viridis* cytoplasmic domain). The vertical bar indicates $A = 0.15$.

strains complemented with mutant RC H genes could have been due to either low levels of the RC formed or to weak catalytic activity of cells replete in a hybrid RC.

Absorption Spectroscopy of ΔPUHAΔPUC Strains Expressing Mutant RC H Genes. The *R. sphaeroides* LH2$^-$ ΔPUHAΔPUC strain was chosen for these experiments because it is deficient in the production of LH2, thus revealing the positions and amplitudes of RC and LH1 peaks that are normally masked by LH2 peaks. Representative primary data are shown in Figure 4, and the cellular content of the RC as indicated by the area under the 804 nm peak (due to the RC accessory BChls) is summarized in Table 2. Exchange of the periplasmic domain (pEVtip) reduced the amount of RC to 21% of the wild-type amount. The RC was not detectable in cells that produced a RC H protein from which most of the periplasmic domain had been deleted (pEΔPeri).

The substitution of the transmembrane domain (encoded by pEVtrans) reduced the amount of RC to 65% of the wild type, and when the periplasmic and the transmembrane domains were simultaneously replaced (pEVPSCB), there was a reduction in the amount of RC to 66% of the wild type. The substitution of the cytoplasmic domain (pEVCSP) resulted in a very low amount of the RC, too little for quantification using this method. The amplitude of the 870 nm LH1 peak was greatly reduced in cells that contained pEΔPeri, slightly reduced in the pEVtrans-containing cells, and slightly increased in the strain that contained pEVPSCB (Figure 5).

Table 2: Summary of RC Levels and Catalytic Activities Measured in Steady-State Absorption Spectra of Intact LH2$^-$ Cells and Flash Spectroscopy of Chromatophores Obtained from LH2$^+$ Cells

plasmid present in LH2$^+$ or LH2$^-$ strains	% 804 nm peak area LH2$^-$ cells[a]	% RC LH2$^+$ chromatophores[b]	% crt bandshift LH2$^+$ chromatophores[b]
pATSHR (wt)	100 (1)	100	100
pEVtip	21 (2)	24	24
pEΔPeri	U[c]	ND[d]	ND
pEVtrans	65 (3)	66	66
pEVPSCB	66 (1)	ND	ND
pEVCSP	U	18	16

[a] Mean of experiments on cells from three independent cultures, with standard deviations in parentheses. [b] Results of one experiment, with variation typically ~10%. [c] Undetectable. [d] Not done.

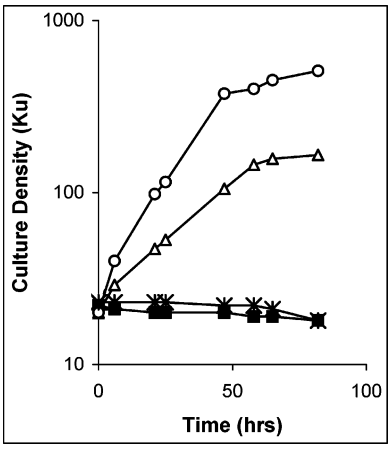

FIGURE 5: Photosynthetic growth of *R. sphaeroides* ΔPUHA (LH2$^+$) cells containing the following plasmids: pATSHR (wild-type RC H, open circles); pEVtip (hybrid RC H containing *B. viridis* periplasmic domain, open triangles); pEVCSP (hybrid RC H containing *B. viridis* cytoplasmic domain, asterisks); and pEΔPeri (mutant RC H lacking the periplasmic domain, filled squares). Ku, Klett units.

Although the amounts of RC indicated by the 804 nm peak area roughly correlate with the photosynthetic growth properties of strains lacking the LH2 complex, it was conceivable that the photosynthetic growth of LH2$^+$ strains that contained these mutant RC H proteins would be different and that the 804 nm peak area does not necessarily indicate the amount of catalytically active RC. Therefore, we turned to a LH2$^+$ background to evaluate photosynthetic growth and used flash spectroscopy to measure the amount of RC and light-driven RC catalytic activity.

Photosynthetic Growth and Flash Spectroscopy of ΔPUHA Strains Expressing Mutant RC H Genes. The relative photosynthetic growth of the RC H mutants in the LH2$^+$ background was similar to the growth of the LH2$^-$ strains, except that the periplasmic domain substitution (pEVtip) supported the growth of LH2$^+$ cells (Figure 5).

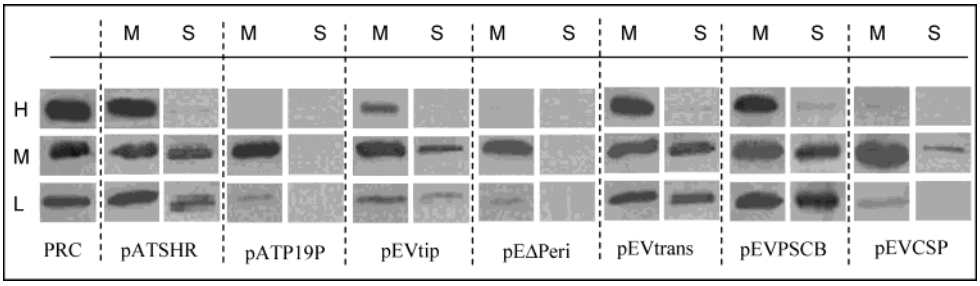

FIGURE 6: Western blot probed with *R. sphaeroides* RC H, RC M, or RC L antibodies. Samples probed were the *R. sphaeroides* purified RC (PRC), and membrane (M) and soluble (S) fractions of ΔPUHAΔPUC cells containing the following plasmids: pATSHR (*R. sphaeroides* RC H); pATP19P (no RC H gene); pEVtip (hybrid RC H containing *B. viridis* periplasmic domain); pEΔPeri (mutant RC H lacking the periplasmic domain); pEVtrans (hybrid RC H containing *B. viridis* transmembrane domain); pEVPSCB (hybrid RC H containing *B. viridis* periplasmic and transmembrane domains); and pEVCSP (hybrid RC H containing *B. viridis* cytoplasmic domain).

The percentage amounts of the RC complex in chromatophores from mutants relative to the wild type, as indicated by photobleaching (due to electron transfer from D to Q_A), are given in Table 2. The values are consistent with the photosynthetic growth properties and the steady-state absorption spectra of LH2$^-$ cells.

The carotenoid bandshift of chromatophores is due to changes in the absorption maxima of carotenoids when an electrochemical potential forms across the chromatophore membrane (*26*). In our experiments, this phenomenon results from light-driven electron and proton-transfer reactions of the RC and cytochrome b/c_1 complexes (*30*). The carotenoid bandshifts of RC H mutants (relative to the wild type) were similar to the relative RC contents detected by photobleaching and absorbance spectra (Table 2).

Taken together, the data indicate that the impairments of photosynthetic growth in these RC H mutants are due to reductions in RC amounts, as opposed to effects on RC catalytic activity, with cellular photosynthetic energy transduction proportional to the amount of RC. This appears to be the case in either the presence or the absence of LH2 (see Discussion).

However, it was not clear whether the reduced RC content was due to a low amount of mutant RC H proteins in cell membranes, resulting in a commensurate reduction in the amount of the RC complex, or if membranes were replete in mutant RC H proteins that were impaired in the assembly of a stable RC complex.

RC H, RC M, and RC L Protein Levels in Membrane and Soluble Cell Fractions. Cells of the ΔPUHAΔPUC strain containing relevant plasmids were disrupted, and fractions probed with antisera directed against RC H, RC M or RC L proteins in Western blots. The amounts of membrane and soluble fractions used were proportional to the nonfractionated cell extracts, and exposure times were chosen to yield the same intensity of a constant amount of a purified RC control. This allows semiquantitative comparisons of the amounts of these three proteins in the two fractions and between different Western blots.

As shown in Figure 6, the *R. sphaeroides* 28 kD band detected by the RC H antiserum was present in membranes of cells containing the wild-type RC H gene (pATSHR), whereas the amount of RC H in the soluble fraction was extremely low. This band was absent from membrane and soluble fractions of the RC H$^-$ strain containing pATP19P. The amount of RC M in membranes of the RC H$^-$ strain was about the same as in the wild-type RC H-complemented strain although, significantly, the amount of membrane-associated RC L was greatly reduced in the absence of the RC H protein. We were surprised to discover substantial amounts of RC M and RC L in the soluble fraction of cells that contained the wild-type RC H protein in the membrane, whereas RC M and RC L were not detected in the soluble fraction of RC H$^-$ cells.

Membrane preparations of cells expressing the RC H periplasmic domain substitution (pEVtip) contained less RC H than the wild-type control, about the same amount of RC M, but less of RC L. The amounts of RC M and RC L in the soluble fraction were lower than in the wild-type RC H control (pATSHR).

Membranes of cells containing the RC H periplasmic domain deletion (pEΔPeri) contained a vanishingly small amount of this mutant RC H protein, the amount of RC M was equivalent to the wild-type control, and the amount of RC L was very low. All three of the RC proteins were undetectable in the soluble fraction.

Membrane and soluble fractions of cells containing the RC H transmembrane domain substitution (pEVtrans) contained about the same amounts of RC H, RC M, and RC L as the wild-type control, as did samples of cells containing the simultaneous exchange of periplasmic and transmembrane domains (pEVPSCB).

The membranes of cells that produced the cytoplasmic domain-substituted RC H (pEVCSP) appeared to contain an extremely low amount of this mutant protein in Western blots probed with the *R. sphaeroides* RC H antiserum. However, it is likely that this polyclonal antiserum reacts predominantly with cytoplasmic domain residues, which in pEVSCP would give a weak signal (as in the experiments on the *B. viridis* preparations; Figure 2B). We suggest that the amount of this hybrid RC H protein in membranes of *R. sphaeroides*, although low, is greater than indicated by the band intensity in Figure 6. The amount of RC M was high, whereas the amount of RC L was low in the membrane fraction, and the amounts of RC L and RC M in the soluble fraction were greatly reduced.

DISCUSSION

In this paper, we report on a protein domain mutagenesis approach to address RC H functions, with a focus on substitution of structurally well-characterized but functionally poorly understood *R. sphaeroides* RC H protein domains with the corresponding *B. viridis* sequences.

This approach arose from genetic complementation experiments on *R. sphaeroides* RC H gene deletion strains that expressed the *B. viridis* RC H gene but were incapable of photosynthetic growth. Because there are several ways to explain these results, we reduced the complexity of analysis by using strains that contained only one or two RC H domain sequence changes, to investigate possible contributions of these individual domains to RC catalytic activity, assembly of the RC complex, and membrane localization of RC proteins.

All of the RC H genes were expressed using the *puc* promoter of pATP19P (*20*), and the RC M and RC L genes were expressed from the wild-type chromosomal *puf* operon. Therefore, we attribute reductions in the steady-state levels of proteins to proteolysis that occurs when RC proteins fail to interact to form the RC complex (*16*).

Periplasmic Domain. Photosynthetic growth was impaired in LH2$^-$ *R. sphaeroides* cells that contained the periplasmic domain replacement and deletion (Figure 3). The absorption spectra in the LH2$^-$ background (Figure 4) and the photobleaching experiments in the LH2$^+$ background (Table 2) indicate that, regardless of the presence of LH2, the amount of the RC complex in these strains is congruent with their photosynthetic growth properties. Because the carotenoid bandshift of these strains was approximately proportional to their RC content, changes in the periplasmic domain of RC H do not seem to affect light-driven electron transfer and proton translocation in the RCs that were assembled. It appears that there is a minimal cellular RC content that supports photosynthetic growth under our conditions (of growth medium, light intensity, etc.), which we estimate to be in the range of 60−70% of the wild-type amount when LH2 is absent and 20−30% of the wild-type amount when LH2 is present.

The Western blot results (Figure 6) show the importance of the periplasmic domain for RC H levels in the membrane fraction and reveal a correspondence between the amount of membrane-associated RC H and membrane-associated RC L but not RC M. For example, the deletion of periplasmic residues 3−10 (pEΔPeri) resulted in only a trace of RC H in the membrane fraction, similar to the complete absence of RC H. In both cases, the amount of membrane-associated RC L was greatly reduced whereas the amount of RC M was about the same as in the wild-type control. When the *R. sphaeroides* RC H periplasmic domain was replaced with the *B. viridis* sequence (pEVtip), the membrane-associated RC H and L proteins were detected at levels lower than the wild-type control, while the amount of RC M in membranes was not reduced. Site-directed mutations of Thr-5 → Val and Asn-9 → Leu, either independently or together, resulted in small decreases in the amounts of RC H protein (data not shown). Thus, it appears that there are several amino acids in the periplasmic domain that together affect RC H (and hence RC L) amounts in the membrane, whereas the amount of membrane-associated RC M is independent of RC H and RC L.

We were surprised to find that in strains which produced the wild-type RC H protein, and hence were replete in all three RC proteins, significant amounts of RC M and RC L (but little RC H) were detected in the soluble fraction of disrupted cells (Figure 6). This result is counter-intuitive, because RC M and RC L are much more hydrophobic than RC H. Cells containing RC H proteins with periplasmic domain mutations that impaired membrane localization contained lower amounts of both RC M and RC L proteins in the soluble fraction. We suggest that the presence of the RC H protein in the membrane, which is in part dependent on the periplasmic domain sequence, is needed to sustain wild-type levels of RC M and RC L proteins in the cytoplasm. Perhaps upon membrane insertion, RC H interacts with one or more RC assembly factors (*12*, *13*, *17*), and this interaction stabilizes newly translated RC M and RC L proteins in a soluble form, for membrane insertion dedicated to RC assembly. This possibility is under investigation.

Transmembrane Domain. In contrast to the periplasmic domain, substitution of the *R. sphaeroides* RC H transmembrane domain with the radically different and one amino acid longer *B. viridis* sequence (Figure 1A) encoded by pEVtrans did not appear to affect membrane localization of RC H or RC L, and RC M was again present at the wild-type level (Figure 6). The amounts of these proteins in the soluble fraction were also similar to the wild-type control. Thus, despite a greatly different amino acid sequence, a stretch of 20−21 amino acids in the α-helical transmembrane domain suffices for RC H and, consequently, RC L accumulation in the membrane. However, there appears to be a secondary role of the RC H transmembrane domain in RC assembly. This is because although the substitution of the transmembrane domain did not greatly affect the amounts of individual RC proteins, it reduced the amount of the RC complex in the membrane to ∼66% of the wild-type control (Table 2), which impaired photosynthetic growth (Figure 3). We attribute this lowering of the RC complex level to an inability of the *B. viridis* transmembrane sequence to properly interact with the *R. sphaeroides* RC M protein.

Analysis of the *R. sphaeroides* RC crystal structure (Brookhaven PDB 1AIJ) indicates that only amino acids of the RC M protein could interact with RC H transmembrane amino acid side chains. RC H transmembrane residues with atoms located ≤3.5 Å of RC M residue atoms are (RC M amino acids given in parentheses) Ser-14 (Trp-297, His-301); Phe-20 (Leu-204); Tyr-30 (Arg-267); Gln-32 (Phe-258); Glu-34 (Arg-267); and Asn-35 (Gly-264, Ile-265, Trp-268). Several of these interactions appear to be hydrogen bonds (e.g., RC H residues Ser-14, Tyr-30, Glu-34, and Asn-35) and so are candidates for determinants of quaternary structure in the *R. sphaeroides* native RC. All of these residues are changed in the transmembrane substitution (Figure 1A).

The carotenoid bandshift of chromatophores containing the transmembrane-substituted RC H was within experimental error proportional to the RC content (Table 2). Therefore, the significance of the RC H/M amino acid interactions discussed above appears to be solely in the assembly of the RC, with little or no effect on RC catalytic activity.

Simultaneous Substitution of Periplasmic and Transmembrane Domains. As noted above, substitution of the *R. sphaeroides* with the *B. viridis* periplasmic domain reduced the amount of RC H in the membrane, whereas the analogous transmembrane substitution did not appear to affect membrane localization. These two domain changes were combined (in plasmid pEVPSCB), resulting in a RC H protein consisting of *B. viridis* sequences from the N-terminus to amino acid Arg-34, followed by the *R. sphaeroides* cytoplasmic domain (Figure 1A).

This simultaneous substitution of periplasmic and transmembrane domains yielded cells with photosynthetic growth properties (Figure 3); RC complex absorption and activity (Figure 4 and Table 2); and amounts of membrane-associated and soluble forms of RC H, RC M, and RC L proteins (Figure 6) that were more like those resulting from the transmembrane than the periplasmic individual substitutions. One way to view these results is that the inhibitory effect of the periplasmic substitution on the level of RC H in the membrane is ameliorated by the addition of the transmembrane substitution. We speculate that species-specific interactions between periplasmic and transmembrane residues enhance RC H accumulation in the membrane.

Cytoplasmic Domain Substitution. A recent crystal structure of the *R. sphaeroides* RC revealed many interactions between RC H/M/L residues and water molecules in the RC H cytoplasmic domain (*31*). Site-directed mutational studies implicated His residues on the surface of the RC H cytoplasmic domain as proton donors to RC M and RC L residues in proton translocation pathways leading to Q_B (*18*−*20*). Therefore, we suspected that the substitution of the *R. sphaeroides* RC H 226 amino acid cytoplasmic domain with the *B. viridis* 223 amino acid domain (∼40% identity) might result in cells that were incapable of photosynthetic growth because of impaired proton translocation. However, the absorption spectra (Figure 4), flash spectroscopy (Table 2), and Western blot experiments (Figure 6) indicate that possible effects of RC H cytoplasmic residue changes on RC catalytic activity are overshadowed by effects on RC assembly. As with the other domain mutations that reduced the amounts of membrane-associated RC H and RC L, and the cytoplasmic amounts of RC M and RC L, there was not a reduction of the amount of RC M in the membrane. We suggest that the RC H cytoplasmic domain also functions to obtain an optimal amount of RC H in the cell membrane, which in turn is needed for accumulation of RC M and RC L in the cytoplasm, and subsequent accumulation of RC L in the membrane for RC assembly.

Interaction between RC and LH1 Complexes. It was suggested that the RC complex is required for maximal amounts of the LH1 complex in several purple bacterial species (*13*−*15*, *17*) and that the N-terminus of LH1 β interacts with the cytoplasmic domain of RC H (*32*). Although this paper is not focused on LH1, we note that LH1 levels were reduced by RC H periplasmic and transmembrane domain mutations (Figure 4).

CONCLUSION

The data in this paper indicate that the RC H mutations that impaired photosynthetic properties did so by reducing the amount of the RC complex in the cell membrane. These effects appear to stem from decreases in the amount of membrane-associated RC H and override possible effects on the catalytic activity of low amounts of RCs that were assembled. The periplasmic and cytoplasmic domain substitutions greatly reduced the amount of membrane-associated RC H, whereas the transmembrane domain substitution functioned well for membrane targeting. All three domains of the RC H protein contain amino acid sequences that are required to obtain wild-type levels of the RC complex in the cell membrane.

It was previously suggested that the *R. sphaeroides* RC H protein has a chaperone-like function in RC assembly, that the amount and stability of RC M in the membrane are dependent on the presence of RC H, and that RC H-stabilized RC M in the membrane leads to productive association of RC M with RC L, resulting in RC assembly (*16*). However, the RC H mutation in the strain used by these authors (in contrast to our RC H mutation) appears to have a polar effect on the expression of genes located 3′ of the RC H gene and deletes part of the 5′ *lhaA* gene (*12*, *14*, *16*, *17*), which we suggest accounts for the reduced amount and rapid degradation of RC M in their experiments. Although we agree that RC assembly requires interactions among all three RC proteins, and that inhibition of these interactions results in proteolysis, our data show that the steady-state amount of membrane-associated RC M protein is independent of RC H. This is in contrast to the amount of membrane-associated RC L, which parallels the amount of the RC H protein, and so the accumulation of RC M in the membrane does not require stoichiometric amounts of RC H or RC L. The rates of accumulation and degradation of RC proteins in our system will be described in a future paper.

The data in this paper indicate a requirement for membrane localization of RC H to obtain substantial amounts of RC M and RC L in the soluble fraction, which were decreased by most of the mutations. We speculate that this unusual accumulation of these two hydrophobic proteins in the cell cytoplasm represents a pool of apoproteins that is used for RC assembly when RC H is present.

We suggest the following scheme to explain our results in the context of RC complex assembly: (1) The RC M protein accumulates in the cell membrane regardless of the presence of RC H or RC L; (2) reductions in the amount of membrane-associated RC H protein results in reductions in RC L (because of proteolysis); (3) the RC H protein, when present, interacts with RC M/L (in part through RC H/M transmembrane sequences), resulting in the stabilization of RC L; and (4) the RC H/M/L interaction results in the accumulation of substantial amounts of RC M and RC L proteins in the cytoplasm, for maximal rates of RC assembly.

ACKNOWLEDGMENT

We thank S. Kaplan and E. Abresch for providing antisera, M. Paddock for purified *R. sphaeroides* RC and discussions, M. Aklujkar for comments on the manuscript, and H. Axelrod for assistance in crystal structure analyses.

REFERENCES

1. Okamura, M. Y., Paddock, M. L., Graige, M. S., and Feher, G. (2000) *Biochim. Biophys. Acta 1458*, 148−163.
2. Woodbury, N. W., and Allen, J. P. (1995) in *Anoxygenic photosynthetic bacteria* (Blankenship, R. E., Madigan, M. T., and Bauer, C. E., Eds.) Kluwer Academic Publishers, Dordrecht, The Netherlands.
3. Prince, R. C. (1990) *Bacteria 12*, 111−149.
4. Blankenship, R. E. (2001) *Molecular Mechanism of Photosynthesis*, Blackwell Science, Oxford.
5. McDermott, G., Prince, S. M., Freer, A. A., Hawthornthwaite-Lawless, A. M., Papiz, M. Z., Cogdell, R. J., and Isaacs, N. W. (1995) *Nature (London) 374*, 517−521.
6. Koepke, J., Hu, X., Muenke, C., Schulten, K., and Michel, H. (1996) *Structure 4*, 581−597.

7. Sundström, V., and Grondelle, R. v. (1995) in *Anoxygenic photosynthetic bacteria* (Blankenship, R. E., Madigan, M. T., and Bauer, C. E., Eds.) pp 349−372, Kluwer Academic Publishers, Dordrecht, The Netherlands.
8. Loach, P. A. (2000) *Proc. Natl. Acad. Sci. U.S.A. 97*, 5016−5018.
9. Verméglio, A., and Joliot, P. (2002) *Biochim. Biophys. Acta 1555*, 60−64.
10. Lancaster, C. R. D., Ermler, U., and Michel, H. (1995) in *Anoxygenic photosynthetic bacteria* (Blankenship, R. E., Madigan, M. T., and Bauer, C. E., Eds.) pp 503−526, Kluwer Academic Publishers, Dordrecht, The Netherlands.
11. Debus, R. J., Feher, G., and Okamura, M. Y. (1985) *Biochemistry 24*, 2488−2500.
12. Chen, X.-Y., Yurkov, V., Paddock, M. L., Okamura, M. Y., and Beatty, J. T. (1998) *Photosynth. Res. 55*, 369−373.
13. Wong, D. K.-H., Collins, W. J., Harmer, A., Lilburn, T. G., and Beatty, J. T. (1996) *J. Bacteriol. 178*, 2334−2342.
14. Sockett, R. E., Donohue, T. J., Varga, A. R., and Kaplan, S. (1989) *J. Bacteriol. 171*, 436−446.
15. Cheng, Y. S., Brantner, C. A., Tsapin, A., and Collins, M. L. P. (2000) *J. Bacteriol. 182*, 1200−1207.
16. Varga, A. R., and Kaplan, S. (1993) *J. Biol. Chem. 268*, 19842−19850.
17. Aklujkar, M., Harmer, A. L., Prince, R. C., and Beatty, J. T. (2000) *J. Bacteriol. 182*, 5440−5447.
18. Ädelroth, P., Paddock, M. L., Tehrani, A., Beatty, J. T., Feher, G., and Okamura, M. Y. (2001) *Biochemistry 40*, 14538−14546.
19. Paddock, M. L., Ädelroth, P., Feher, G., Okamura, M. Y., and Beatty, J. T. (2002) *Biochemistry 41*, 14716−14725.
20. Keller, S., Beatty, J. T., Paddock, M., Breton, J., and Leibl, W. (2001) *Biochemistry 40*, 429−439.
21. Ditta, G., Schmidhauser, T., Yakobsen, E., Lu, P., Liang, X.-W., Finlay, D. R., Guiney, D., and Helinski, D. R. (1985) *Plasmid 13*, 149−153.
22. Beatty, J. T., and Gest, H. (1981) *Arch. Microbiol. 129*, 335−340.
23. Weaver, P. F., Wall, J. D., and Gest, H. (1975) *Arch. Microbiol. 105*, 207−216.
24. Michel, H. (1982) *J. Mol. Biol. 158*, 567−572.
25. Prince, R. C., Davidson, E., Haith, C. E., and Daldal, F. (1986) *Biochemistry 25*, 5208−5214.
26. Jackson, J. B., and Crofts, A. R. (1969) *FEBS Lett. 4*, 185−189.
27. Dutton, P. L., Petty, K. M., Bonner, H. S., and Morse, S. D. (1975) *Biochim. Biophys. Acta 387*, 536−556.
28. Peterson, G. (1983) *Methods Enzymol. 91*, 95−119.
29. Laemmli, D. M. (1970) *Nature (London) 227*, 680−685.
30. Lilburn, T. G., Prince, R. C., and Beatty, J. T. (1995) *J. Bacteriol. 177*, 4593−4600.
31. Abresch, E. C., Stowell, M. H. B., McPhillips, T. M., Rees, D. C., Soltis, S. M., Paddock, M. L., Axelrod, H. L. A., Okamura, M. Y., and Feher, G. (1998) *Photosynth. Res. 55*, 119−125.
32. Conroy, M. J., Westerhuis, W. H. J., Parkes-Loach, P. S., Loach, P. A., Hunter, C. N., and Williamson, M. P. (2000) *J. Mol. Biol. 298*, 83−94.
33. Keen, N. T., Tamaki, S., Kobayashi, D., and Trollinger, D. (1988) *Gene 70*, 191−197.
34. Messing, J. (1983) *Methods Enzymol. 101*, 20−78.

BI0346650